Journal of the European Ceramic Society **15** (1995) 1101–1109
Elsevier Science Limited
Printed in Great Britain
0955-2219(95)00084-4
0955-2219/95/$9.50

At-Temperature Observation of Phase Development in Yttrium α-Sialon

A. Ashkin,[a] D. Ashkin,[a] O. Babushkin[a] & T. Ekström[b*]

[a]Department of Engineering Materials, Luleå University of Technology, S-951 87 Luleå, Sweden
[b]Department of Inorganic Chemistry, Arrhenius Laboratory, Stockholm University, Sweden

(Received 14 February 1995; revised version received 19 May 1995; accepted 22 May 1995)

Abstract

A powder mixture of α-Si_3N_4, AlN and Y_2O_3 corresponding to an yttrium α-sialon composition, $Y_{0.4}Si_{10.2}Al_{1.8}O_{0.6}N_{15.4}$, was sintered both in a high temperature X-ray diffraction unit and in a regular sintering furnace. X-ray analysis was performed and it was shown that high temperature X-ray diffraction can be used to monitor the kinetics of the α-sialon phase formation during sintering at temperatures between 1450 and 1580°C as the reactions take place. A variety of yttrium-rich intermediate and secondary phases are formed during sintering; those formed in the HT-XRD unit were not the same as those formed in the regular sintering furnace, but they do not significantly influence the overall reaction sequence or the amount of α-sialon formed. Quantitative analysis of the acquired data was used to evaluate the kinetics of the α-sialon phase formation; the estimated activation energy of the initial stage α-sialon formation was 330 kJ/mol. After this initial stage of relatively rapid α-sialon formation the process became inhibited.

1 Introduction

The sialons are a group of ceramic compounds corresponding to the α and β form of silicon nitride, in which silicon and nitrogen atoms have been substituted in part by aluminium and oxygen.[1] Unlike α silicon nitride which transforms to β silicon nitride at high temperatures, α sialon can be stabilized by metal ions such as yttrium. The α sialons are characterized by good thermal shock resistance and high hardness which is retained to quite high temperatures.[2] They therefore have potential as materials for high temperature applications.

*Present address: Industrial Research Limited, Lower Hutt, New Zealand.

The present work concerns the formation of a yttrium α-sialon with the ideal composition $Y_{0.4}Si_{10.2}Al_{1.8}O_{0.6}N_{15.4}$ by reactive sintering of an appropriate mixture of silicon nitride, aluminium nitride and yttria powders. This composition is predicted to yield pure α sialon with some glassy phase upon completion of the reaction. Reactions of similar compositions have been studied earlier by means of sintering plus quenching experiments and the general sequence of reactions at temperatures between 1000 and 1750°C has been documented.[3–7] It involves the formation of an oxide liquid and then solution of Si_3N_4 and AlN into it, forming an yttrium-containing oxynitride melt from which α-sialon is precipitated. Besides α-sialon, intermediate and secondary phases like YAM ($Y_4Al_5O_9$), J-ss ($Y_4Al_{2-x}Si_xO_{9-x}N_x$), YAG ($Y_3Al_5O_{12}$) and N-melilite ($Y_2Si_3O_3N_4$) are found depending on temperatures and starting compositions. α-sialon forms at as low a temperature as 1400°C when dissolution of the two nitrides, Si_3N_4 and AlN, becomes significant.[4,6] At this temperature the amount of liquid is still low but it increases with temperature as the extent of the liquid phase field increases. However, for a given temperature the amount of available liquid decreases as the reaction to α-sialon proceeds and yttria, oxygen and aluminum are substituted into the structure.

In studies of crystallization of the intergranular glass phase in sialon ceramics it has been noted that the O/N ratio of both the bulk composition and the liquid phase as well as the temperature play a major role in determining which phases crystallize out.[8,9] The composition, quantity, and viscosity of the liquid phase has also been reported to strongly influence densification.[10] These factors might be expected to complicate the kinetics of α-sialon formation. In the present work, the sensitivity of α-sialon formation to intermediate and secondary phases, sintering conditions and controlled changes in compositions was studied.

The study of phase formation in ceramic materials is often impeded by difficulties in following the course of reactions at elevated temperatures. Generally reactions are studied by 'quenching' a series of samples at different stages of the reaction. This approach is adequate for slower reactions such as those controlled solely by solid state diffusion. If fast transformations occur during cooling, it is hard to retain a high-temperature state unless special experimental conditions are used. For example it has recently been shown that the α-sialon phase with large stabilizing ions decomposes unexpectedly rapidly upon cooling when a liquid phase is present.[11] An alternative to the quenching technique is offered by high temperature X-ray diffraction (HT-XRD). This permits study of reactions as they proceed; the uncertainty associated with quenching is avoided and the kinetics of reactions can be determined far less arduously. A potential drawback of the method is that it can only observe a thin zone of material close to the free surface of a sample which may not give a true representation of realistic bulk sintering conditions. One of the purposes of this work was to apply HT-XRD to a study of the reactions during the sintering of the α-sialon and to compare the observations with the results of conventional sintering.

2 Experimental

Powder mixtures were prepared from the starting materials, silicon nitride (H.C. Starck, Berlin, Grade LC1), aluminum nitride (H.C. Starck, Berlin, Grade A) and yttrium oxide (H.C. Starck, Berlin, Grade > 99·8% Y_2O_3) to correspond to x = 0·4 in the formula $Y_x(Si_{12-4.5x},Al_{4.5x})(O_{1.5x},N_{16-1.5x})$ for yttrium α-sialon (corresponding to 78·0 wt% silicon nitride, 14·4 wt% aluminium nitride and 7·6 wt% yttria). The oxide contents of the aluminum nitride and silicon nitride were compensated for to best approximate the above formula as discussed in a previous article by two of the authors.[12] Samples for the HT-XRD were prepared by cutting powder bodies, CIPed at 200 MPa, into thin slices with a razor, presintering them at 1350°C for 1 h in 0·11 MPa nitrogen atmosphere and then dry grinding them to a dimension of 12 × 8 × 1 mm.

HT-XRD measurements were then conducted at temperatures 1450, 1500, 1530 and 1580°C in a static atmosphere of 0·11 MPa N_2 in a specially constructed graphite furnace coated with silicon nitride. This coating was stable to a temperature of 1600°C. Furnace and HT-XRD conditions have been described earlier.[13] During a soaking time at temperature the reactions were followed by repeating a set of two scans . The first scan over a 2θ range of 28–45° at a rate of 0·04°/s was used to follow the sequence of formation of all phases and to calculate the AlN content by integrating intensities of major peaks. The second scan over a 2θ range of 42–44° and a rate of 0·01°/s was used for profile analysis of one α-Si_3N_4 peak (hkl = 301) and the corresponding peak of α-sialon. These peaks were not overlapped by peaks of other phases and could be used for quantitative estimates of the α-silicon nitride to α-sialon conversion. After the HT-XRD runs, selected samples were analysed by room temerature XRD (RT-XRD) at different depths into the sample to assess any differences between top surface and inner reactions.

Quantitative phase analysis was performed through careful calculation of the XRD peak areas. Correction for overlap of the diffraction peaks as well as the integration of the peak areas were performed by fitting of the experimental diffraction profile using a Marguardt non-linear least squares algorithm.[14] The same algorithm was also used to determine the positions of the α and α' (301) peaks and AlN (101) peak. (α and α' denote α-silicon nitride and α-sialon respectively). The highest accuracy of peak areas and positions was achieved at 1580°C, where the peak separation was largest. The amounts of aluminium nitride, silicon nitride and yttria were estimated by reference to the peaks of an unsintered sample.

The amount of α-sialon was measured in terms of the degree of conversion from α-silicon nitride to α sialon:

$$f = S\alpha'/(S\alpha'+S\alpha) \quad (1)$$

where f is the relative mass fraction α-sialon, $S\alpha'$ the area of the α-sialon (301) peak and $S\alpha$ the area of the α-Si_3N_4 (301) peak. Low amounts of α' were indicated only by an asymmetry of the α peak and therefore required careful deconvolution. It should also be noted that this estimate of the degree of conversion implies that it occurs merely as a crystallographic transformation without any change of composition or change of the total quantity of $\alpha+\alpha'$. Thus the increase in the mass of α' by incorporation of AlN and Y_2O_3 is neglected in the definition of f and consequently the fraction of α' is somewhat overestimated. However, the amounts of AlN and Y_2O_3 involved are relatively small and this approximation has relatively little effect on the values of f obtained. The small amount of β silicon nitride ($\approx$5%) in the starting powder is also disregarded in this analysis.

To verify the HT-XRD results, parallel sintering experiments were conducted in a graphite sintering

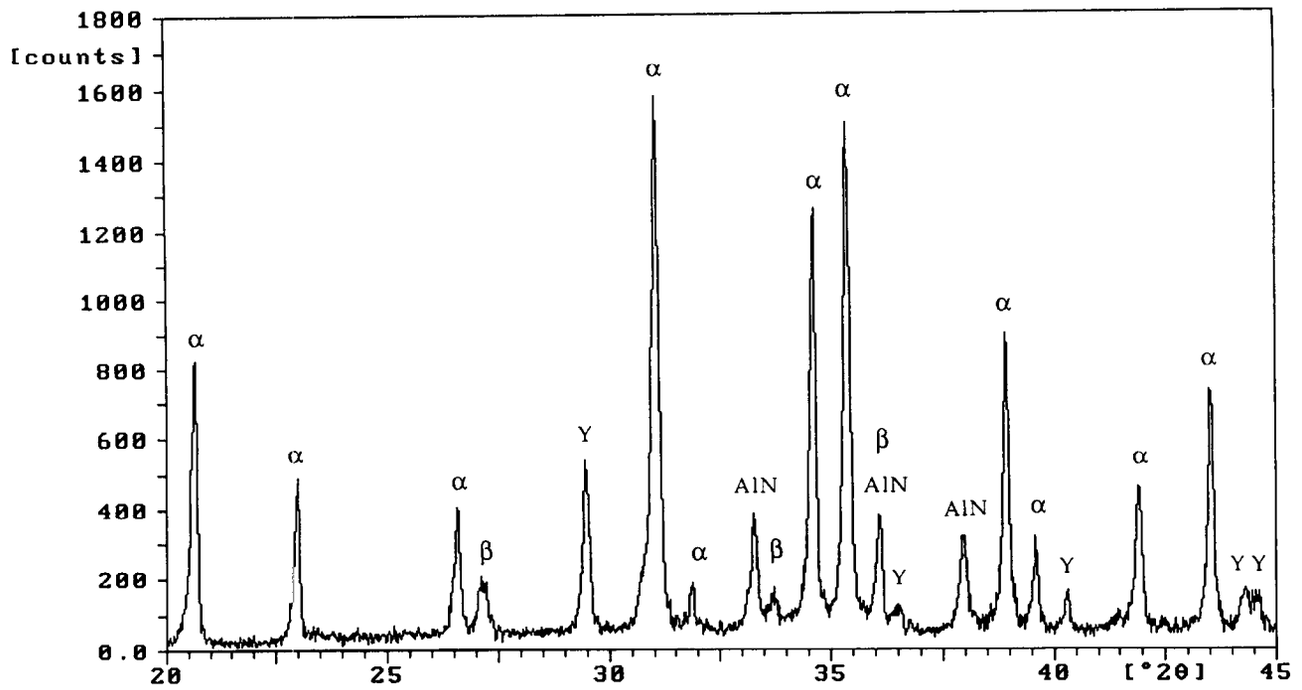

Fig. 1. RT-XRD pattern of sample presintered at 1350°C for 1 h. Where Y = $Y_{10}Al_2Si_3O_{18}N_4$ and/or a J–ss phase ($Y_4Al_{2-x}Si_xO_{9-x}N_x$), and α = α-Si_3N_4 and β = β-Si_3N_4.

furnace with samples of the same composition. Both as-pressed samples and samples presintered as above were sintered at a temperature of 1560°C in 0·15 MPa N_2 for 3 h in a silicon nitride powder bed. All samples were analysed for phase content by XRD at room temperature. The cooling rates between the sintering temperature and 1000°C were approximately 100°C/min in the HT-XRD unit and 20°C/min in the sintering furnace.

In the HT-XRD, the investigated sintering surface is totally open to the furnace atmosphere. To assess the possible effects of this, another two sets of samples were prepared for comparison. In the first set (A) additions of 0·5–3·0 wt% silica were made to the original composition. The second set (B) was given the same nominal composition but with different raw materials. The powders used for the second set of samples had a higher oxide content than those used in the original HT-XRD study and were AlN (H.C. Starck, Berlin Grade B) and Si_3N_4 (Kemanord, Grade P95). The silica used in all the mixtures was derived from an ammonia stabilized colloidal silica, destabilized by propanol. After drying this was easily comminuted to a fine-grained silica by use of an agate spex mill. The atomic composition of the two sets of samples is shown in Table 1. To allow comparison between the two sets, the Al + Si content was adjusted to 12 in the atomic formula. The second set had a higher Si:Al ratio and this was further increased slightly by the addition of silica.

3 Results

3.1 HT-XRD analysis

The XRD diffraction pattern of the original composition presintered for 1 h at 1350°C is shown in Fig. 1. Presintering resulted in formation of yttrium-rich aluminosilicate phase(s) and no detectable α-sialon. The yttrium-rich aluminosilicate phase could be identified as $Y_{10}Al_2Si_3O_{18}N_4$ but

Table 1. Normalized atomic compositions of α-sialon mixtures with different amounts of silica added

	% SiO_2	*Y*	*Al*	*Si*	*O*	*N*
Composition (A)	0	0·400	2·099	9·901	1·099	14·968
	0·5	0·398	2·090	9·910	1·193	14·906
	1	0·397	2·083	9·917	1·287	14·842
	2	0·393	2·064	9·936	1·479	14·721
	3	0·390	2·048	9·952	1·669	14·594
Composition (B)	0	0·404	1·802	10·198	1·286	14·946
	0·5	0·402	1·794	10·206	1·380	14·884
	1	0·400	1·788	10·212	1·475	14·821
	3	0·393	1·754	10·246	1·856	14·572

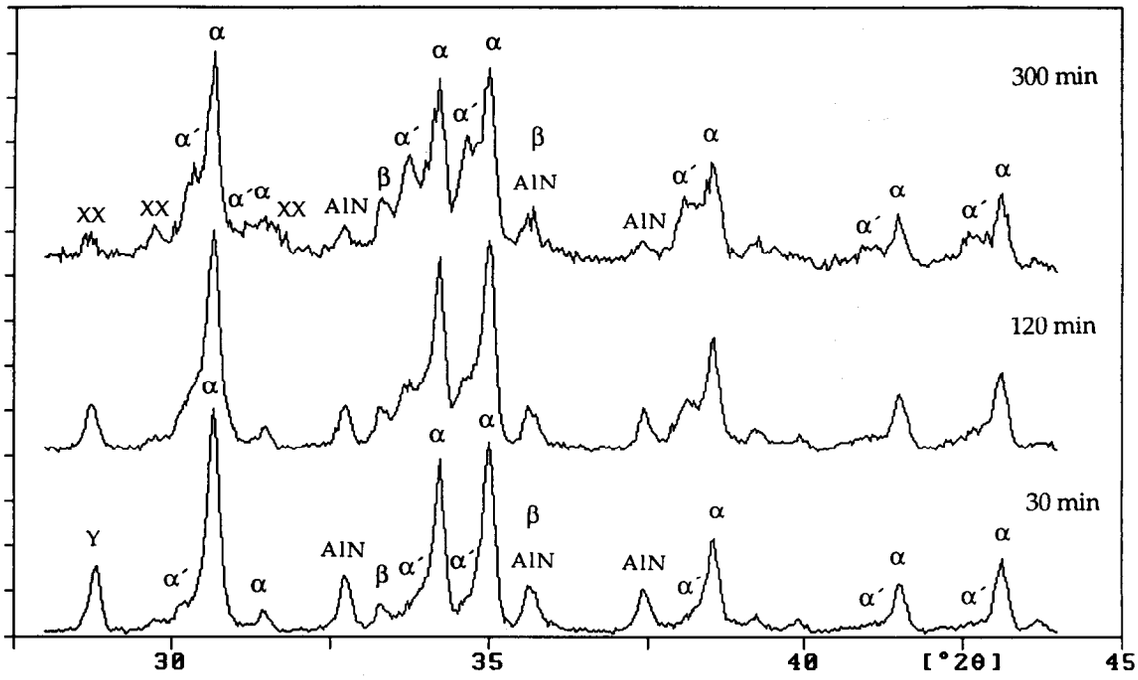

Fig. 2. Phase development with time at 1580°C as-measured at temperature in the HT-XRD, where XX = unidentified secondary phase(s).

with small shifts in the peak positions indicating a shift from stoichiometry or the incorporation of other ions. The major peaks of this phase, however, overlap the peaks of the J–ss phase. Some additional minor diffuse peaks might belong to a J–ss type phase. Their simultaneous presence therefore cannot be excluded. Nevertheless all these phases are characterized by being yttria- and oxygen-rich and will for convenience be denoted $Y_{10}Al_2Si_3O_{18}N_4$ in this paper. The formation of $Y_{10}Al_2Si_3O_{18}N_4$ suggests either the initial formation of an oxynitride melt or a direct reaction between yttria and the oxynitride layers that can be assumed to exist on the surfaces of the Si_3N_4 and AlN powders.

Figure 2 gives an example of how the phase composition develops during sintering in the HT-XRD (at 1580°C in this case). The initial formation of α-sialon was indicated only by an asymmetric broadening of the α-Si_3N_4 peaks. Times up to 5 h were needed for a clear peak shift to occur. Only very small amounts of β-Si_3N_4 could be detected. The evolution of the phase composition with temperature (5 h sintering) as measured at room temperature after sintering in the HT-XRD is summarized in Fig. 3. The results agree well with the HT-XRD measurements as regards the

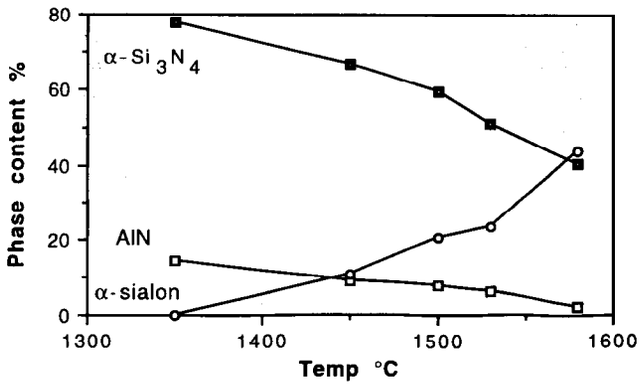

Fig. 3. Amounts of phases measured at room temperature after sintering in the HT-XRD unit for 5 h. The relative amounts of α-sialon and α-Si_3N_4 were calculated from asymmetry of the (301) XRD diffraction peak.

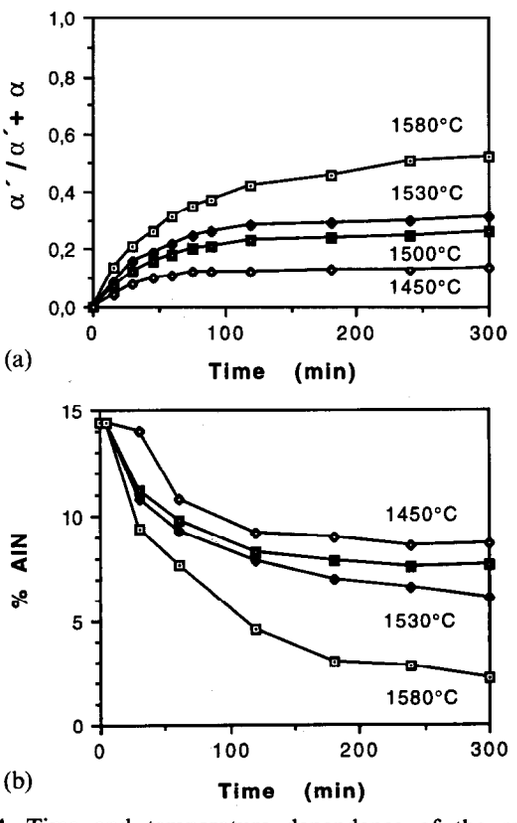

Fig. 4. Time and temperature dependence of the relative amount of (a) α-sialon ($\alpha'/\alpha'+\alpha$) and (b) AlN as-measured at temperature.

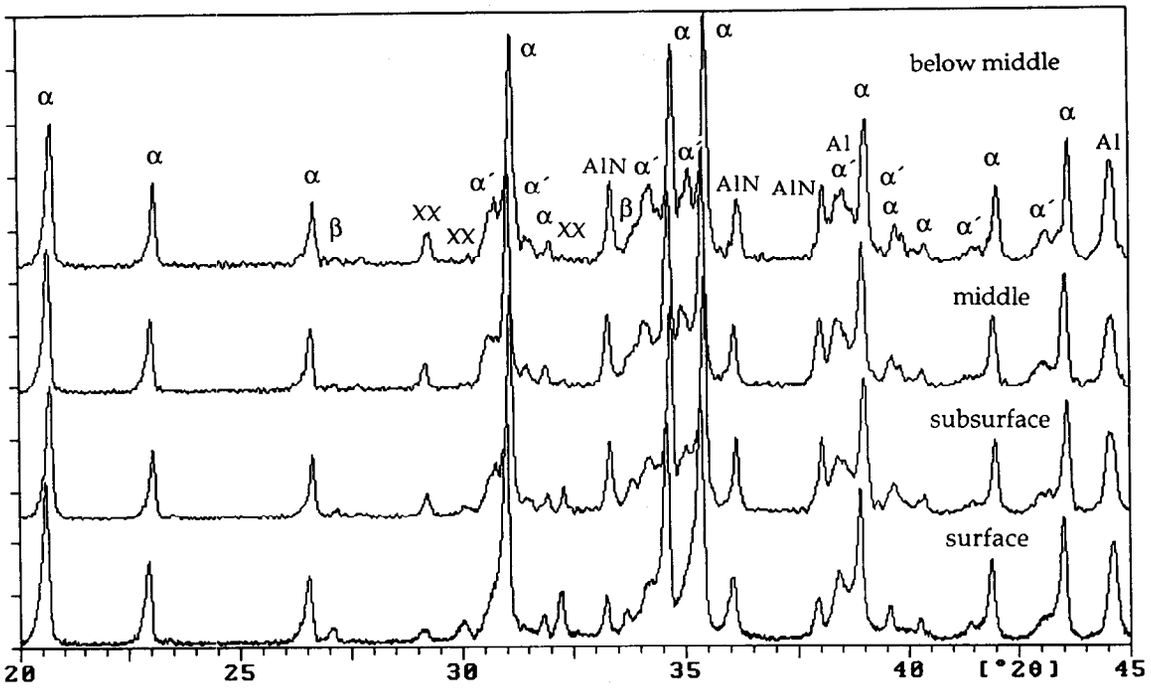

Fig. 5. RT-XRD of sample sintered at 1530°C for 5 h in the HT-XRD at different distances from the surface.

relative amounts of α and α' and with the results of other investigations of α-sialon formation.[5,6] Figures 4(a) and (b) show the increase in α-sialon and decrease of AlN with time at the different sintering temperatures. The trend in rate of formation of α-sialon corresponds well with the trend of the dissolution rate of AlN.

The amount of $Y_{10}Al_2Si_3O_{18}N_4$ was observed to decrease with both time and temperature (*cf.* Fig. 2). Instead, another phase, or possibly two phases, are formed. These are difficult to identify as they do not fit well with any single known pattern. They could however be based on a solid solution of yttrium silicates or yttrium aluminosilicates, similar to the J–ss phase or apatite.

Figure 5 shows RT diffraction patterns taken at different distances from the surface of the sample subjected to HT-XRD investigation for 5 h at 1530°C, while Table 2 shows the phase composition at corresponding distances for samples studied at different temperatures. The amounts of silicon nitride, α-sialon and $Y_{10}Al_2Si_3O_{18}N_4$ did not seem to differ significantly between the surface and the interior, except in the 1450°C sample, where the level of $Y_{10}Al_2Si_3O_{18}N_4$ is lower on the surface of the sample. The aluminum nitride content on the other hand is consistently higher in the interior. The reduced aluminum nitride content on the surface of the sample is probably due to its having a higher susceptibility to oxidation than silicon nitride. The surface of the sample showed some evidence of glassy phase after HT-XRD.

Although the differences in the amounts of α-sialon between the surface and the interior were small the nature of the α-sialon peaks was different. The peaks on the surface were broader and showed smaller separation from the α-Si_3N_4 peak than those in the interior. This was especially true for the 1530°C samples in which the peak separation in the interior was much larger than at any other temperature investigated (Table 2). This result can be compared with results reported by Walls *et al.*,[6] which showed that the cell parameters of the α-sialon are higher at the beginning of α-sialon formation than at equilibrium. They attributed this to a lower dissolution of silicon nitride than aluminum nitride in the liquid at the beginning of α-sialon formation, allowing a more highly substituted sialon to form. In this investigation the higher peak separation in the interior of the samples coincided with higher amounts of unreacted AlN than were observed at the surface. This implies that AlN does oxidize on the surface

Table 2. Relative amounts (wt fractions) of α-sialon and AlN and the α-sialon/α-Si_3N_4 peak separation at the surface and in the interior of samples sintered 5 h at different temperatures in the HT-XRD unit

Temp°C	*Position*	α'/α + α'	α'–α (2Θ) *separation*	AlN
1450	Surface	0·15	—	0·085
1450	Middle	0·14	—	0·124
1500	Surface	0.31	—	0·08
1530	Surface	0·39	0·434	0·06
1530	Subsurface	0·30	0·520	0·09
1530	Middle	0·31	0·537	0·1
1530	Below middle	0·32	0·525	0·095
1580	Surface	0·52	0·414	0·02
1580	Middle	0·47	0·442	0·06

of the sample and that this influences the peak separation, while the amount α-sialon formed does not change significantly.

3.2 Conventionally sintered compositions

As explained above, samples of the same composition as those studied in HT-XRD were sintered in a powder bed in a conventional furnace. First, a comparison was made between samples pressed directly from powders and samples presintered at 1350°C with the HT-XRD samples. There was no detectable difference in the overall phase composition of the two samples.

A difference, however, was found between the surface and interior of the conventionally sintered samples. The surface consisted of α- and β-Si_3N_4 and YAG, while the interior contained α-sialon, N-melilite, unreacted α-Si_3N_4 and AlN. The samples had also gained weight slightly ($\approx$ 1%) during sintering. This implies a mass transfer from the powder bed to the sample probably caused by a higher partial pressure of oxygen or silicon monoxide in the powder bed. The reduced AlN content on the surface of HT-XRD samples suggests that a similar effect occurred in the HT-XRD unit.

Figure 6 compares the room temperature phase composition of the interior of presintered + conventionally sintered sample sintered at 1560°C with the surface compositions of presintered + HT-XRD sintered samples treated at 1530 and 1580°C. It is seen that the α-sialon content of the interior of the sample sintered at 1560°C is similar to that of the surface of the 1580°C HT-XRD sample. The intermediate phases in the HT-XRD sample were however different from those both in the surface and interior of the conventionally-sintered sample. In the 1530°C HT-XRD sample the α-Si_3N_4 to α-sialon conversion had not proceeded as far but the yttrium-rich intermediate phase(s) is the same as in the 1580°C HT-XRD sample. These experiments show that the furnace coating in the HT-XRD unit provides a reasonable atmosphere for the sample but does not interact with the sample in the same way as a powder bed.

3.3 Conventionally sintered compositions with silica additions

Since the observed decrease in AlN content on the surfaces of the HT-XRD and conventionally sintered samples might be attributed to an oxidation, it was of interest to see how an increase in oxide content of the starting compositions would influence the phase formation. The two sets of samples shown in Table 1 were sintered at 1560°C for this purpose.

Table 3 shows the room temperature phase contents of the cross sections of the different sets of samples with 0·5 to 3·0 wt% extra silica. For (A) samples, i.e. those based on the original mixture, the phase composition comprised α-sialon, melilite, β-Si_3N_4 and unreacted Si_3N_4 and AlN; with increasing silica content, the YAG phase began to develop and the fraction of melilite decreased. In the (B) samples, based on the comparison composition, the development was very similar but instead of melilite the $Y_{10}Al_2Si_3O_{18}N_4$ phase formed; moreover it disappeared faster than the melilite in the (A) samples. The amount of α-sialon was not significantly affected, except for the 3% silica addition samples in set (B).

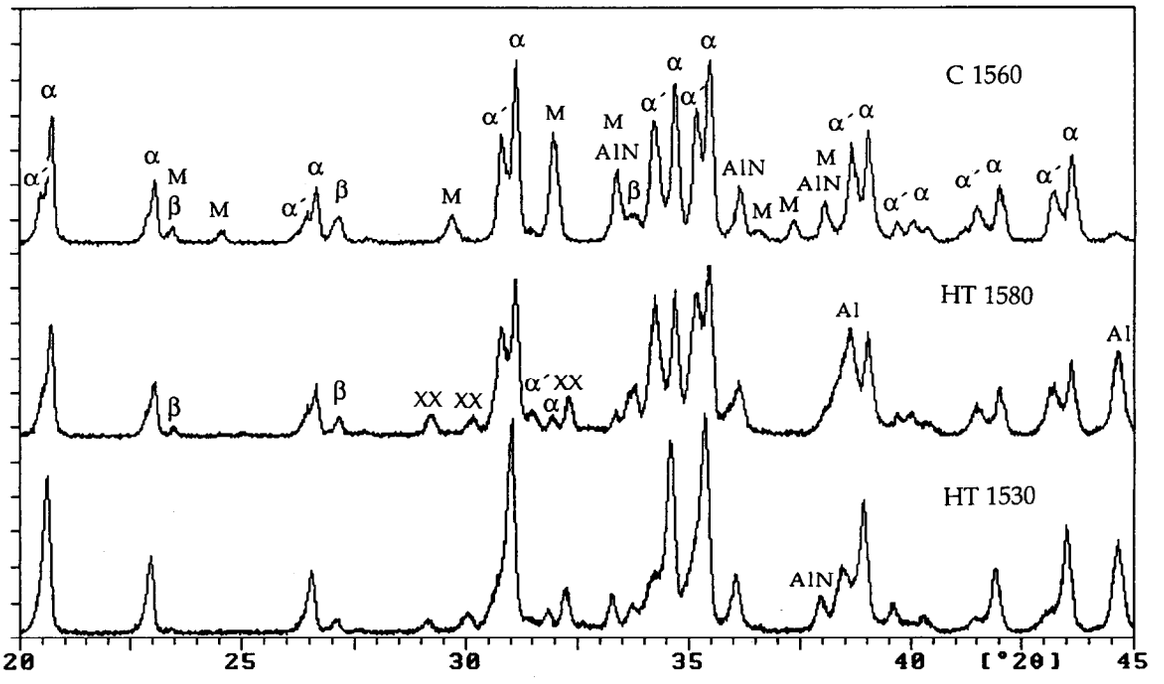

Fig. 6. RT-XRD patterns of samples presintered at 1350°C and then sintered at 1560°C in a conventional furnace (C1560), at 1530°C in the HT-XRD (HT1530) and at 1580°C in the HT-XRD (HT1580). M = $Y_2Si_3N_4O_3$.

Table 3. Phase compositions of conventionally sintered samples as a function of silica additions. Series A is the original HT-XRD composition and series B the comparison composition. α = α-Si_3N_4, α' = α-sialon, β = β-sialon, M = N–melilite, Y = $Y_{10}Al_2Si_3O_{18}N_4$. Brackets indicate very small amounts

Composition	*Phases observed*	*α–α' shift(2θ)*	*α'/α + α'*
A/0%SiO_2	α/α'/β/M/AlN	0·359	0·31
A/0·5%SiO_2	α/α'/β/M/AlN	0·375	0·35
A/1%SiO_2	α/α'/β/M/AlN	0·381	0.38
A/2%SiO_2	α/α'/β/M/YAG/AlN	0·369	0·37
A/3%SiO_2	α/α'/β/(M)/YAG/AlN	0·371	0·39
B/0%SiO_2	α/α'/β/Y/(YAG)/AlN	0·372	0·46
B/0.5%SiO_2	α/α'/β/(Y)/YAG/AlN	0·367	0·44
B/1%SiO_2	α/α'/β/YAG/AlN	0·358	0·42
B/3%SiO_2	α/α'/β/YAG/AlN	0·292	0·30

The most significant effect observed when slightly increasing the O/N-ratio of both series of samples, were the changes in the yttrium-rich intermediate phases that formed. Nitrogen-rich melilite in the A-series samples and $Y_{10}Al_2Si_3O_{18}N_4$ in the B-series gave way to oxygen-rich YAG as the overall oxygen content of the material increased.

3.4 Kinetics of α-sialon formation

The above sintering experiments showed that within the range of sintering conditions used here the degree of conversion to α-sialon is not very sensitive to small changes in oxygen content or to the intermediate phases formed. It is therefore possible to use the HT-XRD data to examine the kinetics of α-sialon formation under these circumstances. The isothermal plots of sialon formation in Fig. 4(a) show that the conversion rate is greatest within the first 90–120 min of the sintering, decreasing markedly at longer times. The reaction is considered to occur by dissolution and transport of the reactants in the liquid oxide phase and the formation of the α-sialon at the surfaces of α-Si_3N_4. The inhibition of the reaction could occur by a decrease in the fraction of the liquid phase, necessitating increased degree of solid state diffusion, or covering of silicon nitride surfaces. To describe the rapid early stage of the process, only the first period of 120 min was used in determining a reaction rate constant. In this stage the transformation was assumed to be described by a simple reaction law:

$$df/dt = k(1 - f)^n \qquad (2)$$

where n is the index of reaction, f the fraction of α sialon formed and k the reaction rate constant. To evaluate the results, a best-fit n-value was determined for the 1580°C data. It was then assumed that the reaction mechanism for all other temperatures was the same and consequently this n-value (3·64) was used to estimate the k values for all temperatures. The k values thus derived are 0·0023 (1450°C), 0·0045 (1500°C), 0·0061 (1530°C) and 0·0102 (1580°C). Reaction curves based on the above assumption are drawn in Fig 7(a) and indicate the extent to which the assumed kinetic description is reasonable. The temperature dependence of the reaction rate is expressed in the form of an Arrhenius diagram in Fig. 7(b) and yields an effective activation constant of 330 kJ mol^{-1} which is consistent with a liquid diffusion process.

An alternative approach to determining the activation energy, requiring no assumptions about the process kinetics, is to construct an Arrhenius plot on the basis of ln $1/t$ versus $1/T$ where t is the time required to give a fixed degree of reaction. Here a satisfactory linear relationship was achieved for t corresponding to a conversion of 10% and this confirmed the activation constant of 330 kJ mol^{-1}. This corresponded to a reaction time

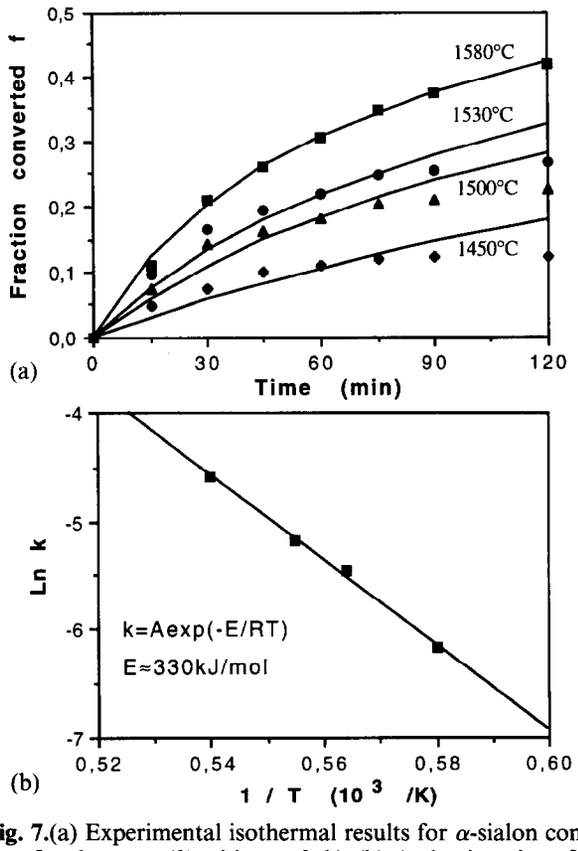

Fig. 7.(a) Experimental isothermal results for α-sialon conversion fitted to eqn (2) with n = 3·64; (b) Arrhenius plot of rate constants derived from 7(a).

of 45 min at 1450°C. Beyond this time, the results for 1450°C were no longer consistent with the linear Arrhenius plot implying an inhibiting change in reaction mechanism.

4 Discussion

As already indicated, the reaction sintering of the material studied here occurs by a complex combination of associated mechanisms occurring both in parallel and in series. After formation of an oxide liquid from surface oxides and yttria these mechanisms will include dissolution of AlN and α-Si_3N_4, transport of reactant atoms through the liquid, formation of sialon on the α-Si_3N_4 and subsequently solid state diffusion of reactants through the sialon. In addition a number of intermediate and secondary phases form depending on sintering conditions and composition. A microstructural study by Hwang *et al.*[15] has indicated that α-sialon formation occurs predominantly by heterogeneous nucleation and preferential growth on undissolved silicon nitride grains.

One of the interesting aspects of this investigation is that in the range of temperatures and conditions studied the rate and extent of α-sialon formation was relatively insensitive to small changes in oxygen content and was not influenced by the intermediate phases formed. Thus the α-sialon formation was determined mainly by the temperature and time. This is in accordance with previous findings. For example, Cao *et al.*[16] in studying the effect of extra alumina additions to an α-sialon composition concluded that, while densification was affected by the liquid phase, the early formation of α-sialon was not significantly influenced by small changes in the composition, amount or the viscosity of the liquid. The intermediate phase that formed changed from melilite to YAG with addition of alumina, but this did not influence the overall reaction sequence.

In the present work, the fact that the amount of α-sialon did not seem to change significantly with small changes in composition, while the peak separation did, suggests that the number of growing α-sialon grains was fairly constant at a given temperature but that its composition could vary. The rate of sialon formation is probably determined by the rate of dissolution and transport of silicon nitride and AlN, and therefore strongly dependent on temperature. The lower availability of AlN on the surface of the HT-XRD samples on the other hand probably only leads to a lower substitution of the α-sialon and does not affect the number and growth of grains.

β-Si_3N_4 only seem to form in very small amounts at the temperatures studied here unless major compositional changes occur, for example through a significant increase in oxygen activity, as on the surface of a sample in contact with a powder bed containing only silicon nitride and silica. It is therefore likely that the α-sialon has the lowest energy of formation at high nitrogen activities and at these relatively high temperatures. It has been suggested in the past that the α-Si_3N_4 structure is a low-temperature modification, but with yttria stabilization it readily forms.

The above observations imply that, although small compositional changes on an open surface are unavoidable, high-temperature X-ray diffraction is still an appropriate method to study the kinetics of α-sialon formation or decomposition. On the other hand, HT-XRD may not always be suitable as a means of monitoring all the products of the reactions since the intermediate and secondary phases are strongly dependent on sintering conditions. Thus, in the present study the $Y_{10}Al_2Si_3O_{18}N_4$ formed during presintering gradually disappeared during treatment in the HT-XRD while other intermediary phases formed. These were different from those formed during sintering in a powder bed in a conventional graphite furnace.

A very characteristic feature of the kinetics of sialon formation was the dramatic inhibition of growth after a certain fraction of transformation. The range of inhibition moved to higher fractions of transformation and longer times with increasing temperature suggesting that the effect may be caused by a decrease in the amount of liquid.

5 Conclusions

The reaction sintering of an yttria α-sialon from a mixture of yttria, AlN and α-Si_3N_4 has been studied at temperatures between 1450 and 1580°C. The rate of α-sialon formation was significant during an initial reaction stage but became inhibited after a limited fraction of conversion had occurred. The rate of reaction as well as the fraction of conversion and time at which inhibition set in all increased with temperature. The activation energy of the initial reaction stage was 330 kJ/mol.

A variety of intermediate and secondary phases were observed to form during sintering depending on variations in the sintering conditions such as the oxygen level of the sintering environment and small variations in the starting composition. The rates of α-sialon formation were however not affected significantly by these variations in conditions or secondary phases.

Since the rate of α-sialon formation is relatively insensitive to other sintering conditions than the

temperature, HT-XRD is considered to be a suitable technique for studying the kinetics of α-sialon formation and was applied for this purpose in this study. The technique is however considered unsuitable for the study of the formation of secondary phases since these are very sensitive to the sintering conditions.

Acknowledgements

The authors extend thanks to Professor Richard Warren for valuable advice. The work was supported financially by The Research Council of Norrbotten. T. Ekström acknowledges the support of the Swedish Research Council for Engineering Sciences.

References

1. Jack, K. H. & Wilson, W. I., Ceramics based on the Si–Al–O–N and related systems. *Nature, Phys. Sci.*, **238** (1972) 28–9.
2. Cao, G. Z. & Metselaar, R., α'-Sialon ceramics: A review. *Chem. Mater.*, **3** (1991) 242–52.
3. Nagel, A., Greil, P. & Petzow, G., Reaction sintering of yttrium containing α-silicon nitride solid solution. *Revue de Chimie Minérale*, **22** (1985) 437–48.
4. Ishizawa, K., Ayuzawa, N., Shiranita, A., Takai, M., Uchida, N. & Mitomo, M., Some properties of α-sialon ceramics. In *Proc. Ceramic Materials and Components for Engines*, eds W. Bunk & H. Hausner. Deutsche Keramische Gesellschaft, 1986, pp. 511–18.
5. Slasor, S. & Thompson, D. P., Preparation and characterisation of yttrium α'-sialons. In *Proc. Non-oxide Technical and Engineering Ceramics*, Limerick, Ireland, 1985, pp. 223.
6. Walls, P. A. & Thompson, D. P., Reaction mechanisms in the formation of calcium and yttria α'-β'sialon composites. In *Br. Ceram. Proc. Special Ceramics.*, **8**, 1986, pp. 35–50.
7. Cao, G. Z., Metselaar, R. & Ziegler, G., Preparation and properties of α' and α' + β'-sialon ceramics. *Mater. Forum*, **16** (1992) 299.
8. Winder, S. M. & Lewis, M. H., Nitrogen content of the intergranular glass phase in syalon ceramics. *J. Mater. Sci. Lett.*, **4** (1985) 241–3.
9. Mandal, H., Thompson, D. P. & Ekström, T., Heat-treatment of Ln–Si–Al–O–N glasses. *Key Engin. Mater.*, **72–74** (1992) 187.
10. Cao, G. Z., Metselaar, R. & Ziegler, G., Formation and densification of α'-sialon ceramics. *Material Science Monographs*, 66B, ed. P. Vincenzini, Amsterdam, 1991, pp. 1285–93.
11. Mandal, H., Thompson, D. P. & Ekström, T., Reversible α↔β sialon transformation in heat-treated sialon ceramics. *J. Eur. Ceram. Soc.*, **12** (1993) 421.
12. Bartek, A., Ekström, T., Herbertsson, H. & Johansson, T., Yttrium α-sialon ceramics by hot isostatic pressing and post-hot isostatic pressing. *J. Am. Ceram. Soc.*, **75** (1992) 432–9.
13. Ashkin, A., Ashkin, D. & Babushkin, O., Investigation of α-sialon formation by high temperature X-ray diffraction. In *Proc. Int. Conf. on Silicon Nitride Based Ceramics*, Trans Tech Publications, Switzerland, eds M. J. Hoffmann, P. F. Becher & G. Petzow, 1993, pp. 373–7.
14. Schreiner, W. N. & Jenkins, R., *Adv. X-ray Anal.*, **26** (1983) 141–8.
15. Hwang, S. L. & Chen, I. W., Nucleation and growth of α'-sialon on α-Si_3N_4. *J. Am. Ceram. Soc.*, **77** (1994) 1711–18.
16. Cao, G. Z., Metselaar, R. & Ziegler, G., Effects of the characteristics of silicon nitride powders on the preparation of α'-sialon ceramics. *J. Mater. Sci. Lett.*, **11** (1992) 1685.